International Journal of Multidisciplinary and Current Research

Research Article

ISSN: 2321-3124
Available at: http://ijmcr.com

Post-Buckling Analysis of FGM Beams According to Different Shear Deformation Theories

Alireza Daneshmehra[a], Mohsen Heydaria[a] and **Majid Akbarzadeh Khorshidia[a]**

[a]School of Mechanical Engineering, College of Engineering, University of Tehran; Tehran, Iran.

Accepted 01 July 2013, Available online 01 August 2013, (**July/Aug 2013 issue)**

Abstract

In this paper, the compact solution for post-buckling of beam made of functionally graded material under axial loading is introduced. The FGM beam ends are restrained from axial movement. The governing equations and the boundary conditions are derived using the principle of stationary potential energy and the governing equations are solved by closed-form method. The effects of material compositions, slenderness ratios and boundary conditions that lead to the considerable changes in buckling and post-buckling behaviors are investigated. The shear deformation effects on the critical buckling load is introduced using Euler-Bernoulli, Timoshenko, and some higher-order beam theories. Results of this analysis illustrate that classical and first-order theories underestimate the amplitude of buckling, while some higher-order theories yield very close results for the static post-buckling response.

Keywords: *FGM; Post-buckling; Shear deformation; Stationary potential energy; beam.*

1. Introduction

The concept of functionally graded materials (FGMs) was first introduced in 1984 by a group of material scientists in Japan [1]. FGMs are novel, microscopically inhomogeneous in which the mechanical properties vary smoothly and continuously from one surface to another. It has many good performances in engineering applications, such as high resistance to large temperature gradients, reduction of stress concentration and so on. Therefore, FGMs have found extensive applications in spacecrafts, space vehicles, nuclear reactors and other situations where large temperature gradients are encountered.

There are many two dimensional theories that have been proposed to account for the shear deformation of moderately deep structures and highly anisotropic composite. Reddy [2] imposed the boundary conditions of transverse shear stresses on top and bottom surfaces of plate and proposed a higher order theory with parabolic distribution of transverse shear stresses across the thickness involving five unknown variables. Touratier [3] proposed a trigonometric shear deformation plate theory where the transverse strain distribution is given as a sine function. Soldatos [4] proposed a hyperbolic shear deformation plate theory. Further, Soldatos and Timarci [5] formulated a general theory that unifies most of the variationally consistent classical and shear deformable cylindrical shell theories. Karama *et al.* [6] proposed an exponential variation for the transverse strain in their study of the bending of composite beams.

Bending analysis of FG beams based on higher order shear deformation under ambient temperature was investigated by Kadoli *et al.* [7]. Xiang and Yang [8] used Timoshenko beam theory to study the free and forced vibration of laminated FG beams under heat conduction using the differential quadrature method (DQM). An analytical solution for free vibration analysis based on the first order shear deformation theory of FG beams was presented by Sina *et al.* [9]. Free vibration and buckling analysis of FG beams, which have an open crack at their edge, were considered by using Euler–Bernoulli beam theory and the rotational spring model by Yang and Chen [10]. The Timoshenko beam theory was employed to study post-buckling and nonlinear vibration of edge cracked FG beams without thermal effects by Ke *et al.* [11] and Kitipornchai *et al.* [12]. An improved third order shear deformation theory has recently been developed by Shi [13] for the problems in which the transverse shear plays an important role. Shi presented static analysis of orthotropic plates based on the improved theory, which provides more accuracy in results than other theories, especially for shear stress prediction.

Samir A.Emam [14] evaluated shear deformable composite beams in post-buckling that presents an exact solution for the static post-buckling response of a

symmetrically laminated simply supported shear-deformable composite beam. Li and Batra [15] proposed Analytical relations between the critical buckling load of a functionally graded material (FGM) Timoshenko beam and that of the corresponding homogeneous Euler–Bernoulli beam subjected to axial compressive load. Most recently, Grover *et al.* [16] proposed a new inverse hyperbolic shear deformation theory for static and buckling analysis of laminated composite and sandwich plates. Meiche *et al.* [17] proposed a new hyperbolic shear deformation theory for buckling and vibration analysis of functionally graded sandwich plates. Mantari *et al.* [18,19] proposed new shear strain functions and presented the analytical solution for laminated and sandwich plates.

The objective of present study is to investigate the significance of the shear deformation of FGM beams under static post-buckling response. The classical, first-order, and some higher-order shear deformation beam theories is employed, and the closed-form solutions are presented for simply supported (H-H) and clamped-clamped (C-C) boundary conditions. The effects of material compositions, slenderness ratios and boundary conditions that lead to the considerable changes in buckling and post-buckling behaviors are investigated. Finally, the critical load of buckling is obtained for higher-order beam theories and is compared with acquired results of the classical and first-order beam theories.

2. Functionally Graded Materials

A FG beam made by ceramic–metal is considered in this investigation. The geometrical properties of beam are shown in Fig. 1. It is assumed that the material properties of the form, *P* (such as the Young's modulus, (*E*), the thermal expansion coefficient (*α*), and density (*ρ*)), which are used to calculate the material stiffness and the moment of inertia for FGMs, can be presented as:

$$P(z) = (P_m - P_c)(\frac{h-2z}{2h})^k + P_c \qquad (1)$$

Where the subscripts 'm' and 'c' denote the metallic and ceramic constituents, respectively, and *z* is the coordinate in the thickness direction (*– h/2 ≤ z ≤ h/2*).

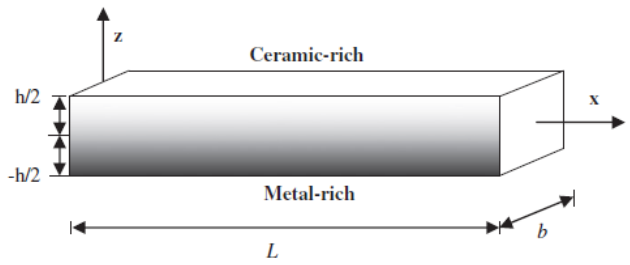

Fig. 1. Geometry of FG beam

It is noted that the positive real number *k* ($0 < k \le \infty$) is the power law index, and *z* is the distance from the mid-plane of the FG beam. The volume fractions of the constituent materials, which are assumed to be ceramic of volume V_c and metal of volume, V_m may be expressed using the power law distribution as [20]:

$$V_m = 1 - V_c, V_c = (\frac{1}{2} + \frac{z}{h})^k \qquad (2)$$

Where *h* is the thickness of the beam and *z* is the thickness coordinate measured from the middle surface of the beam. Note that for the upper surface, which is ceramic rich, $V_c(\frac{h}{2}) = 1$ and for the lower surface, which is metal rich, $V_c(\frac{-h}{2}) = 0$. Variation of V_c with *k* and *z/h* is shown in Fig. 2.

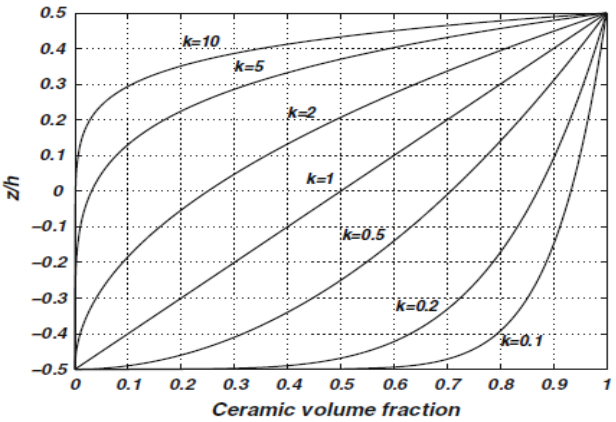

Fig. 2 Variation of ceramic volume fraction with power law index and thickness coordinate

The value of *k* equal to zero represents a fully ceramic beam ($V_c = 1$) and *k* equal to infinity represents a fully metallic beam ($V_c = 0$).

3. Formulation

We consider a FG beam of length *L* and height *h* that is subjected to a compressive axial load $\bar{N}$. The axial and lateral displacements *u* and *w*, respectively, of a point that is at a height *z* measured from the mid-plane and a distance *x* along the beam span in its deformed state are assumed as follows:

$$u(x,z) = u_0(x) - zw' + f(z)\varphi(x) \qquad (3)$$

$$w(x,z) = w_0(x) \qquad (4)$$

Where u_0, w_0 and φ are unknown displacement functions of the mid-plane, with this suppose that beam deformation occurs in *x-z* plane. Also, *f(z)* is a shape function describing the shear deformation across the thickness and the dash designates a partial differentiation with respect to the spatial coordinate x. Table 1 presents the function *f(z)* according to different beam theories [21].

Table 1. *f(z)* describing for Euler-Bernoulli and Timoshenko and higher-order beam theories.

Beam theory	**f(z)**
Classical theory: Euler-Bernoulli	f(z)=0
First-order theory: Timoshenko	f(z)=z
Higher-order theories: Reddy	$f(z) = z - \frac{4z^3}{3h^2}$
Touratier	$f(z) = \frac{h}{\pi}\sin(\frac{\pi z}{h})$
Karama et al.	$f(z) = ze^{\frac{-2z^2}{h^2}}$
Soldatos	$f(z) = h\sinh(\frac{z}{h}) - z\cosh(\frac{1}{2})$
Aydogdu	$f(z) = z\alpha^{\frac{-2(\frac{z}{h})^2}{\ln\alpha}}, \alpha = 3$
Mantari	$f(z) = \sin(\frac{\pi z}{h})$
N. Grover et al.	$f(z) = \sinh^{-1}(\frac{rz}{h}), r = 3$

The small normal strain and the transverse shear strain are given as follows:

$$\varepsilon_x = \frac{\partial u}{\partial x} + \frac{1}{2}(\frac{\partial w}{\partial x})^2 = u' + \frac{1}{2}w'^2 - zw'' + f(z)\varphi' \tag{5}$$

$$\gamma_{xz} = \frac{\partial w}{\partial x} + \frac{\partial u}{\partial z} = f'(z)\varphi \tag{6}$$

The relationships between stresses and strains in the form of elastic constitutive equations are:

$$\sigma_x = Q_{11}(z)\varepsilon_x \tag{7}$$

$$\tau_{xz} = Q_{55}(z)\gamma_{xz} \tag{8}$$

The elastic constants for FG beams varied continuously through the beam thickness can be expressed as:

$$Q_{11}(z) = \frac{E(z)}{1-\nu^2} \tag{9}$$

$$Q_{55}(z) = G(z) = \frac{E(z)}{2(1+\nu)} \tag{10}$$

The stress resultants are introduced as follow:

$$N_x = \iint \sigma_x dydz, M_x = \iint z\sigma_x dydz, P_x^s = \iint f(z)\sigma_x dydz, Q_x^s = \iint f'(z)\tau_{xz} dydz \tag{11}$$

Where N_x and M_x are the force and moment stress resultants, P_x^s and Q_x^s are stress resultants due to shear deformation. To simplify the Eq. (11), the material stiffness components are used.

$$\begin{bmatrix} N_x & M_x & P_x^s \end{bmatrix}^T = \begin{bmatrix} A_{11} & B_{11} & E_{11} \\ B_{11} & D_{11} & F_{11} \\ E_{11} & F_{11} & H_{11} \end{bmatrix} \begin{bmatrix} u' + \frac{1}{2}w'^2 & -w'' & \varphi' \end{bmatrix}^T \tag{12a}$$

$$Q_x^s = A_{55}\varphi' \tag{12b}$$

The extensional stiffness A_{11}, bending-coupling stiffness B_{11}, bending stiffness D_{11}, warping extensional coupling stiffness E_{11}, warping-bending coupling stiffness F_{11}, and warping-higher order bending coupling stiffness H_{11} are used into Eq. (12) and A_{55} is associated with shear stiffness components [9]. All of the stiffness components can be expressed as:

$$A_{11}, B_{11}, E_{11}, D_{11}, F_{11}, H_{11} = \iint Q_{11}(z)(1, z, f(z), z^2, zf(z), f^2(z))dydz \tag{13a}$$

$$A_{55} = \iint Q_{55}(z) f'^2(z) dydz \tag{13b}$$

The total potential energy can be expressed as follows:

$$U = \frac{1}{2}\iiint (\sigma_x \dot{o}_x + \tau_{xz}\gamma_{xz})dydzdx + \frac{1}{2}\int_0^L \bar{N}w'^2 dx \tag{14}$$

Where $\bar{N}$ is the external load applied on the beam along the *x* axis. Substituting Eqs. (5)-(6) and (11) into Eq. (12), the total potential energy is obtained.

$$U = \frac{1}{2}\int_0^L [N_x(u' + \frac{1}{2}w'^2) - M_x w'' + P_x^s\varphi + \bar{N}w'^2]dx \tag{15}$$

4. Solution

The governing equations are achieved by using the principle of stationary potential energy.

$$\delta U = 0 \tag{16}$$

Where δ is the first variation.

The natural and essential boundary conditions are acquired by Eq. (14), that the essential boundary conditions are the same governing equations. These equations are introduced as follow:

$$\frac{dN_x}{dx} = 0 \tag{17a}$$

$$\frac{d^2M_x}{dx^2} + \frac{d}{dx}(N_x w') - \bar{N}\frac{d^2w}{dx^2} = 0 \tag{17b}$$

$$\frac{dP_x^s}{dx} - Q_x^s = 0 \tag{17c}$$

Substituting Eq. (12) into Eq. (17), the governing equations can be expressed as follow:

$$A_{11}(u' + \frac{1}{2}w'^2)' - B_{11}w''' + E_{11}\varphi'' = 0 \tag{18a}$$

$$A_{11}[(u' + \frac{1}{2}w'^2)w']' + B_{11}u''' + E_{11}(w'\varphi')' + F_{11}\varphi''' - D_{11}w'''' - \bar{N}w'' = 0 \tag{18b}$$

$$E_{11}(u' + \frac{1}{2}w'^2)' - F_{11}w''' + H_{11}\varphi'' - A_{55}\varphi = 0 \tag{18c}$$

By twice integrating of the Eq. (18a) with respect to the spatial coordinate *x*, the axial displacement versus other variations is obtained.

$$u(x) = -\frac{1}{2}\int_0^x w'^2 dx + \frac{B_{11}}{A_{11}}w' - \frac{E_{11}}{A_{11}}\varphi + \frac{c_1}{A_{11}}x + c_2 \tag{19}$$

Where c_1 and c_2 are constants of integral, which can be determined from the boundary conditions. The boundary conditions for clamped beam are as follows:

$$u(0) = u(L) = w'(0) = w'(L) = 0 \tag{20}$$

As is known, placing the boundary conditions into the Eq. (19) constants c_1 and c_2 are determined.

$$c_2 = \frac{E_{11}}{A_{11}}\varphi(0) \tag{21a}$$

$$c_1 = \frac{A_{11}}{2L}\int_0^x w'^2 dx + \frac{E_{11}}{L}[\varphi(L) - \varphi(0)] \tag{21b}$$

Now, Eq. (19) comes in the following forms:

$$u(x) = -\frac{1}{2}\int_0^x w'^2 dx + \frac{B_{11}}{A_{11}}w' - \frac{E_{11}}{A_{11}}\varphi + (\frac{1}{2L}(\int_0^x w'^2 dx) + \frac{E_{11}}{A_{11}L}[\varphi(L) - \varphi(0)])x + \frac{E_{11}}{A_{11}}\varphi(0) \tag{22}$$

For clamped-clamped boundary condition, the following displacement field is assumed [22]:

$$w(x) = \cos(\frac{2\pi x}{L}) - 1 \tag{23a}$$

$$\varphi(x) = s\cos(\frac{2\pi x}{L}) - 1 \tag{23b}$$

Where *s* is unknown to be determined. By substituting Eqs. (22) and (23) into Eq. (18b), and solving the resultant equation for $\bar{N}$, the function of critical buckling load versus *h* is obtained for clamped-clamped beam boundary condition.

Now, for simply supported beam, the following displacement field is assumed for the first buckling mode [18]:

$$w(x) = \alpha\sin(\pi\frac{x}{L}) \tag{24a}$$

$$\varphi(x) = \beta\cos(\pi\frac{x}{L}) \tag{24b}$$

Where α and β are unknowns to be determined. Now, by substituting Eqs. (22) and (24) into governing equations, a system of two equation with two unknowns α and ρ is obtained. This system has a non-zero response when determinant of coefficients matrix is zero. By solving this determinant, an equation is formed that can be calculated critical buckling load by using this equation.

$$\begin{bmatrix} \frac{\pi^2}{L^4}(\bar{N}L^2 - D_{11}\pi^2) & \frac{\pi^3 F_{11}}{L^3} \\ \frac{\pi^3 F_{11}}{L^3} & -\frac{H_{11}\pi^2 L + A_{55}L^3}{L^3} \end{bmatrix}\begin{bmatrix}\alpha\\ \beta\end{bmatrix} = \begin{bmatrix}0\\0\end{bmatrix} \tag{25}$$

$$\begin{vmatrix} \frac{\pi^2}{L^4}(\bar{N}L^2 - D_{11}\pi^2) & \frac{\pi^3 F_{11}}{L^3} \\ \frac{\pi^3 F_{11}}{L^3} & -\frac{H_{11}\pi^2 L + A_{55}L^3}{L^3} \end{vmatrix} = 0 \tag{26}$$

Then, critical buckling load:

$$N_{cr} = \frac{\pi}{L^2}(D_{11} - \frac{\pi^2 F_{11}^2}{L^2 A_{55} + \pi^2 H_{11}}) \tag{27}$$

The non-dimensional critical buckling load N_{cr}^*, is defined as follows:

$$N_{cr}^* = \frac{L^2}{Bh^3 E_m}N_{cr} \tag{28}$$

Also, by solving the above system of two equation with two unknowns, the unknowns α and β can be obtained, where α (intensity of displacement in direction *z*) is expressed as the buckling amplitude.

$$\alpha = \frac{2}{\pi\sqrt{A_{11}}}\sqrt{\bar{N}L^2 - \pi^2 D_{11} + \frac{\pi^4 F_{11}^2}{L^2 A_{55} + \pi^2 H_{11}}} \quad (29)$$

Variations of the buckling amplitude versus buckling load, is known as static post-buckling response.

5. Numerical results

The post-buckling response of high-order shear deformable FG beams is not available in the open literature; hence, the validation study for the theoretical formulation in this paper is achieved by comparing the results with those presented in Ref [18]. So, we consider a FG beam that composed of ceramic (alumina) and metal (aluminum) with $E_c = 380GPa$ and $E_c = 70GPa$, respectively, and $\nu = 0.23$ [18].

We use the model developed in the present study to determine the non-dimensional first critical buckling loads for FG beam with different length-to-thickness ratios and compare them with other results in literature. Table 2 presents the non-dimensional critical buckling loads in this study.

It is worth investigating the significance of shear deformation, not only on the critical buckling load but also on the resulting of post-buckling response. The post-buckling response of simply supported FG beams using Euler-Bernoulli's beam theory, Timoshenko's theory and some higher-order shear deformation theories is presented. The variation of the non-dimensional buckling amplitude α^* with the applied non-dimensional critical axial load N^*_{cr} is investigated while the length-to-thickness ratio is varying. Fig. 3 presents the variation of the mid-span post-buckling amplitude with the applied axial load. These figures show that length-to-thickness

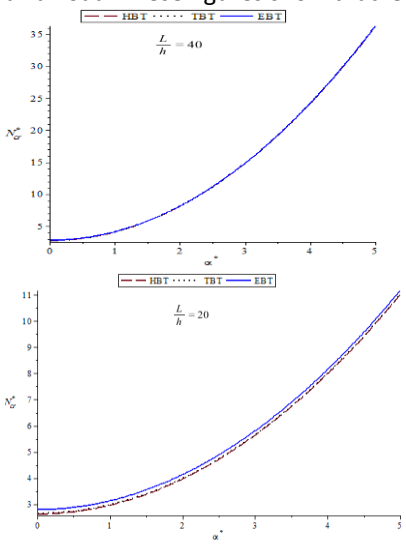

ratio is an important parameter in the analysis of post-buckling of FG beams. As the higher-order shear deformation theories show very close results in the course of the critical buckling load, they also yield similar post-buckling response. We also note that the first-order shear deformation theory always underestimates the amplitude of buckling compared with higher-order theories. For the high length-to-thickness ratios, the shear deformation effect can be neglected.

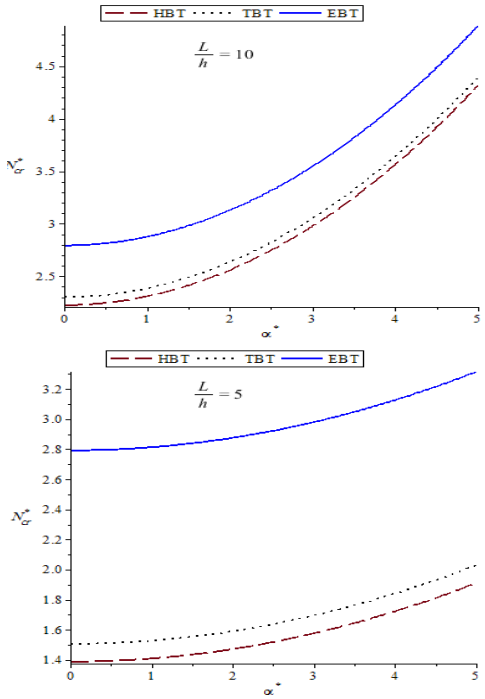

Fig. 3 Variation of the maximum buckling with the applied axial load for $\frac{L}{h} = 40, 20, 10, 5$.

Table 2. Non-dimensional first critical buckling load using different beam theories

Beam theories	L/h			
	5	10	20	40
Euler–Bernoulli	2.791	2.791	2.791	2.791
Timoshenko	2.572	2.733	2.776	2.788
Reddy	2.532	2.722	2.774	2.787
Touratier	2.532	2.722	2.774	2.787
Karama et al.	2.534	2.722	2.774	2.787
Aydogdu	2.534	2.722	2.774	2.787
Soldatos	2.532	2.722	2.774	2.787
Mantari	2.532	2.722	2.774	2.787
N. Grover et al.	2.546	2.726	2.775	2.787

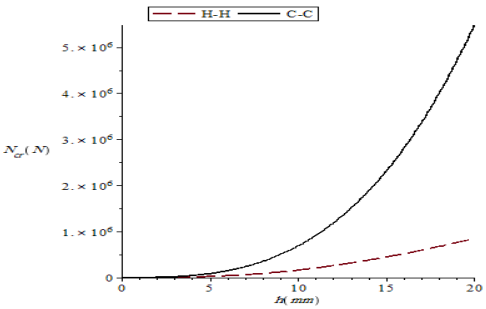

Fig. 4 Variation of critical buckling load with beam thickness

Fig. 4 presents the variation of critical buckling load with beam thickness for simply supported and clamped-clamped boundary conditions. This figure shows that the beam with clamped-clamped boundary condition, bear higher axial load versus simply supported boundary condition.

Fig. 5 and Fig. 6 demonstrate the influence of the power law index *k* on the buckling load of simply supported and clamped-clamped FG beams, respectively. By increasing the power law index, the critical buckling load decreases.

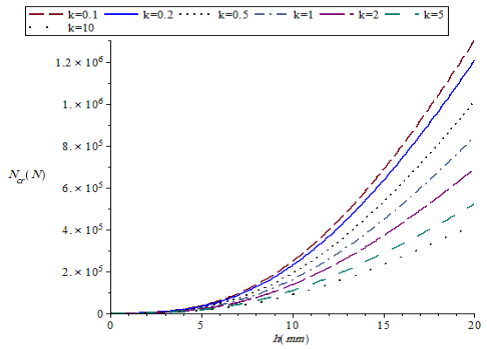

Fig. 5 Critical buckling load versus thickness *h*, for different power law index *k* (H-H boundary condition)

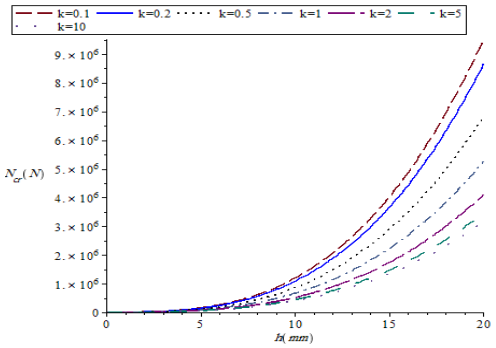

Fig. 6 Critical buckling load versus thickness *h*, for different power law index *k* (C-C boundary condition)

6. Conclusions

The comparison of post-buckling behavior of a FGM beam based on some higher-order shear deformation theories, classical and first-order theories is investigated. The governing equations and the boundary conditions are derived using the principle of stationary potential energy and the governing equations are solved by closed-form method. The effects of material compositions, slenderness ratios and boundary conditions that lead to the considerable changes in buckling and post-buckling behaviors are investigated. From numerical results for simply supported FG beam, we note that the higher-order shear deformation theories show very close results in the course of the critical buckling load, they also yield similar post-buckling response. We also note that the classical and first-order shear deformation theories usually underestimates the amplitude of buckling compared with higher-order theories. For the high length-to-thickness ratios, the shear deformation effects can be neglected.

Additionally, the comparison of critical buckling load of simply supported and clamped-clamped beam is presented, that the clamped-clamped beam can bear more axial load. Also, variation of critical buckling load with different power law indexes is investigated, and we note that by increasing the power law index, the critical buckling load decreases.

References

[1]. M. Koizumi, and M. Niino (1995), Overview of FGM research in Japan, MRS Bull, vol. 20, pp. 19-21.

[2]. J. N. Reddy (1984), A simple higher-order theory for laminated composite plates, J. Appl. Mech., **vol.** 51, pp. 745-752.

[3]. M. Touratier (1991), An efficient standard plate theory, Int. J. Eng. Sci., vol. 29, pp. 901-916.

[4]. K. P. Soldatos (1991), A transverse shear deformation theory for homogeneous monoclinic plates, Acta Mech., vol. 94, pp. 195-200.

[5]. K. P. Soldatos, and T. Timarci (1993), A unified formulation of laminated composites, shear deformation, five-degrees-of-freedom cylindrical shell theories, Compos. Struct., vol. 25, pp. 165-171.

[6]. M. Karama, K. S. Afaq, and S. Mistou (2003), Mechanical behavior of laminated composite beam by new multi-layered laminated composite structures model with transverse shear stress continuity, Int. J. Solids struct., vol. 40, pp. 1525-1546.

[7]. R. Kadoli, K. Akhtar, and N. Ganesan (2008), Static analysis of functionally graded beams using higher order shear deformation theory, Appl. Math. Model., vol. 32, pp. 2509-2525.

[8]. H. J. Xiang, and J. Yang (2008), Free and forced vibration of laminated FGM Timoshenko beam of variable thickness under heat conduction, Compos. Part B Eng., vol. 39, pp. 292-303.

[9]. S. A. Sina, H. M. Navazi, and H. Haddadpour (2009), An analytical method for free vibration analysis of functionally graded beams, Mater. Des., vol. 30, pp. 741-747.

[10]. J. Yang, and Y. Chen (2008), Free vibration and buckling analysis of functionally graded beams with edge cracks, Compos. Struct., vol. 83, pp. 48-60.

[11]. L. L. Ke, J. Yang, and S. Kitipornachai (2009), Postbuckling analysis of edge cracked functionally graded beams under end shortening, Compos. Struct., vol. 90, pp. 152-160.

[12]. S. Kitipornachai, L. L. Ke, J. Yang, and Y. Xiang (2009), Nonlinear vibration of edge cracked functionally graded Timoshenko beams, J. Sound Vib., vol. 324, pp. 962-982.

[13]. G. Shi (2007), A new simple third order shear deformation theory of plates, Int. J. Solids Struct., vol. 44, pp. 4399-4417.

[14]. S. A. Emam (2011), Analysis of shear deformable composite beam in post-buckling, Compos. Struct., vol. 94, pp. 24-30.

[15]. Li. Shi-Rong, and R. Batra (2013), Relations between buckling loads of functionally graded Timoshenko and homogeneous Euler-Bernoulli beams, Compos. Struct., vol. 95, pp. 5-9.

[16]. N. Grover, D. K. Maiti, and B. N. Singh (2013), A new inverse hyperbolic shear deformation theory for static and buckling analysis of laminated composite and sandwich plates, Compos. Struct., vol. 95, pp. 667-675.

[17]. N. E. Meiche, A. Tounsi, N. Zlane, I. Mechab, and E. A. A. Bedia (2011), Anew hyperbolic shear deformation theory for buckling and vibration of functionally graded sandwich plates, Int. J. Mech. Sci., vol. 53, pp. 237-247.

[18]. J. L. Mantari, A. S. Oktem, and C. G. Soares (2012), A new higher order shear deformation theory for sandwich and composite laminated plates, Compos. Part B., vol. 43, pp. 1489-1499.

[19]. J. L. Mantari, A. S. Oktem, and C. G. Soares (2012), A new trigonometric shear deformation theory for isotropic, laminated composite and sandwich plates, Int. J. Solids Struct., vol. 49, pp.43-53.

[20]. N. Wattanasakulpong, B. P. Gangadhara, and D. W. Kelly (2011), Thermal buckling and elastic vibration of third order shear deformable functionally graded beams, Int. J. Mech. Sci., vol. 53, pp. 734-743.

[21]. M. Aydogdu (2009), A new shear deformation theory for laminated composite plates, Compos. Struct., vol. 89, pp. 94-101.

[22]. A. M. Waas (1992), Initial post-buckling behavior of shear deformable symmetrically laminated beams, Int. J. Non-Linear Mech., vol. 27, pp. 817-832.